

¹ **A new finite-frequency shear-velocity model of the European-Mediterranean region**

D. Peter¹, L. Boschi¹, F. Deschamps¹, B. Fry¹, G. Ekström², and D.

Giardini¹

D. Peter, Institute of Geophysics, ETH Zurich, 8093 Zurich, Switzerland.

(dpeter@erdw.ethz.ch)

¹Institute of Geophysics, ETH Zurich,

Switzerland.

²Lamont-Doherty Earth Observatory,

Columbia University, Palisades, NY 10964,

USA.

3 We invert a global phase-anomaly database of intermediate- to long-period
4 Rayleigh waves, recently updated with increased coverage in the European-
5 Mediterranean region, on a global scale with a higher resolution parameter-
6 ization in the region of interest. We first compare phase-velocity inversions
7 based on ray and finite-frequency theory and derive for each a correspond-
8 ing set of local phase-velocity dispersion curves (one per model pixel) between
9 35 s to 300 s period. Effects of the two different theories on the three-dimensional
10 upper-mantle structure are investigated by inverting each dispersion curve
11 for radial shear-velocity profiles. The combination of a gradient-descent method
12 and a random-Monte-Carlo model search provides an estimated shear-velocity
13 model with associated uncertainties for depths between 40 km to 400 km.
14 While differences between ray-theoretical and finite-frequency models are small
15 compared to model uncertainty, comparisons with independent models fa-
16 vor the finite-frequency one.

1. Introduction

In view of current plans to build a European seismological reference model [*Ritzwoller et al.*, 2006], a new surface-wave dataset was assembled [*Fry et al.*, 2008], achieving unprecedentedly dense coverage of the continent. The dataset combines global and regional observations, which helps to further constrain regional seismic models (see e.g. [*Shapiro and Ritzwoller*, 2002]). Tectonics in Europe and in the Mediterranean region are governed by a complex interaction of the African, Eurasian and Arabian plates, comprehensively investigated in several tomographic studies [*Spakman et al.*, 1993; *Wortel and Spakman*, 2001; *Piromallo and Morelli*, 2003; *Boschi et al.*, 2004; *Marone et al.*, 2004; *Fry*, 2007; *Schmid et al.*, 2008;]. Recent phase-velocity models of the region, found using analytical finite-frequency sensitivity kernels, show some significant discrepancies with ray-theoretical ones, especially between the Southern Apennines and the Hellenic Arc [*Fry et al.*, 2008].

It is unclear how such differences in phase-velocity distributions reflect differences in the underlying seismic structures. Identifying a one-dimensional seismic velocity profile from a local dispersion curve is a nonlinear, non-unique problem [*Knopoff*, 1972]. An exploration of the solution space more thorough than those afforded by linearized inversions becomes therefore necessary, to identify a most likely seismic profile and estimate its uniqueness. Focusing on the well sampled European-Mediterranean region [*Fry et al.*, 2008], we use Rayleigh-wave phase-velocity maps derived by both ray and numerical finite-frequency theory [*Peter et al.*, 2007] to build a new set of dispersion curves which, in a second step,

are inverted for radial V_s (shear velocity) profiles. We then compare the resulting three-dimensional shear-velocity models with earlier studies of the region's seismic structure.

2. Data

The global dispersion database of *Ekström et al.* [1997], updated by *Boschi and Ekström* [2002], was further expanded by *Fry* [2007], applying the same measurement technique as *Ekström et al.* [1997] to recordings of both Love and Rayleigh waves from MidSEA, SDSNet, TomoCH and GRSN stations [see *Fry et al.*, 2008, and references therein]. This results in a particularly dense coverage over Europe and the Mediterranean Basin. We invert a total of 677,234 measurements of Rayleigh waves at all available periods between 35s and 300s and epicentral distances between 15° and 165°, and for both minor and major arcs.

3. Method

We invert for local phase velocities with a global multiple-resolution parameterization, where Europe and the Mediterranean region are parameterized with blocks of approximately equal size of 1° x 1°, everywhere else by 3° x 3° blocks. At each period from 35 s to 300 s, we use a least-squares algorithm [*Paige and Saunders*, 1982] to find a phase-velocity map derived by both ray- and finite-frequency theory. For the latter, we computed sensitivity kernels entirely numerically as described and illustrated by *Peter et al.* [2007], in the assumption that the Earth structure be relatively smooth. Our choice of solution is based on an analysis of the L-curves after deriving sets of solution models with different strength of the smoothness damping constraint (no other regularization was applied). For

56 each theory, we compare the inversion solutions corresponding to points of equal curvature
 57 on the L-curve [Peter *et al.*, 2007].

58 Dispersion curves derived from these phase-velocity maps are assembled for each in-
 59 version pixel within Europe and the Mediterranean region (900 locations total). At each
 60 pixel, we next invert the corresponding dispersion curve to find V_s in six distinct layers
 61 (40 - 60 km, 60 - 100 km, 100 - 150 km, 150 - 220 km, 220 - 310 km and 310 - 400 km).

62 In the assumption of a perfectly elastic upper mantle (i.e., neglect of attenuation), we use
 63 Knopoff's method [Schwab and Knopoff, 1970], to calculate a synthetic dispersion curve
 64 for each seismic profile generated by our search algorithm. The search algorithm consists
 65 of a gradient-descent inversion [Tarantola, 2005] subsequently refined by a Monte-Carlo
 66 search.

67 The starting seismic profile combines PREM [Dziewonski and Anderson, 1981] vertically
 68 polarized V_s , compressional velocity V_p , and density for the mantle together with a crustal
 69 description from Crust-2.0 [Bassin *et al.*, 2000], where ocean and Moho depths have been
 70 interpolated from the more detailed ones given in the European crustal model EuCrust-07
 71 [Tesauro *et al.*, 2008].

72 In the Monte-Carlo refinement, we generate $\sim 10^5$ radial profiles by randomly perturbing
 73 the values of V_s at each layer up to 10%, while keeping density and P-velocity fixed
 74 [Deschamps *et al.*, 2008]. Limited to some locations, we verified that even after increasing
 75 the number of sampled solutions to $\sim 10^7$, our final result remains stable.

Our cost function χ^2 , accounting for the observational error σ_j (estimated by Ekström
et al. [1997] and converted to phase velocity) at each period T_j and for the difference

between “observed” $c_{obs}(T_j)$ and computed $c(T_j)$ phase-velocity, is defined as:

$$\chi^2 = \sum_j \frac{[c_{obs}(T_j) - c(T_j)]^2}{\sigma_j^2} + \eta \sum_j \frac{[c'_{obs}(T_j) - c'(T_j)]^2}{\sigma_j^2},$$

where ' denotes derivation with respect to period and η acts as a weighting parameter for the second term, chosen so that the shapes and offsets of the dispersion curves are fit equally well. For all solution profiles for which the phase-velocities lie within one standard deviation of the observational error, we calculate a probability p that depends on the corresponding χ^2 value:

$$p = k e^{-\frac{\chi^2}{2}}$$

where k is a normalization constant. Our final preferred profile coincides with the weighted (with weight p) average of all those profiles, accompanied by the corresponding standard deviations [Deschamps *et al.*, 2008].

4. Results

Figure 1 shows examples of our phase-velocity maps at four different periods (40 s, 75 s, 150 s and 250 s) with important discrepancies between ray- and finite-frequency-theory-derived maps visible for longer periods at 150 s and 250 s [Fry *et al.*, 2008]. Although the sensitivity of Rayleigh waves at the shortest period we consider (35 s) has highest sensitivity mostly below the Moho [Boschi and Ekström, 2002], their sensitivity to the crust is still considerable. We constructed an artificial V_s profile, with crustal layers derived from Crust-2.0 and EuCrust-07 but an artificial upper mantle, and computed a corresponding “synthetic” dispersion curve by Knopoff’s method. We then inverted this synthetic dispersion curve with starting profiles different from the original “input” model. Figure 2a illustrates results of two such tests with crustal structure fixed either to PREM

89 crust or to our crustal model based on Crust-2.0 and EuCrust-07 (as was used to generate
90 the synthetics). It is clear that (i) even if the starting model for the inversion is very wrong
91 (gray dashed line) the input model can be retrieved properly, but (ii) only if the crustal
92 model is reliable. In the absence of an accurate crustal model, retrieved upper-mantle
93 structure is dubious down to ~ 200 km depth.

94 The three-dimensional models derived by ray and finite-frequency theory exhibit differ-
95 ences under Southern Italy and the Hellenic arc at depths between 150 - 400 km. Figure
96 2b shows one of the V_s profiles from the “observed” dispersion curves derived by finite-
97 frequency or ray theory for a location in Southern Italy (41.5°N , 16.5°E). In both cases,
98 crustal structure is fixed to our crustal model based on Crust-2.0 and EuCrust-07. Be-
99 tween 60 km and 100 km, both models show a positive anomaly, which at 100 - 150 km
100 changes to a low-velocity layer. The inversion of the finite-frequency dispersion curve
101 shows higher anomalies at depths between 150 - 310 km. Figure 3 and Figure 4 combine
102 all the V_s perturbations (and their standard deviations) found as described. Standard
103 deviations grow with depth and vary up to 6%, which indicates a decreased resolving
104 power in the dispersion curves.

5. Discussion

105 Comparisons between our ray-theoretical and finite-frequency results confirm the im-
106 portant differences pointed out by Fry et al. [2008]. At the longest periods, our finite-
107 frequency maps exhibit stronger anomalies than those derived by Fry et al. [2008] via
108 analytical finite-frequency kernels. We additionally find that the crustal structure plays
109 an important role in the correct determination of the uppermost ~ 200 km of the radial

¹¹⁰ V_s profiles, confirming the findings of *Waldhauser et al.* [2002]. Including shorter surface-
¹¹¹ wave periods from noise correlations could allow us to extend our model search and invert
¹¹² simultaneously for crustal layer parameters [*Panza et al.*, 2007]. In both V_s -models (Fig-
¹¹³ ure 3) we find the same prominent features as *Boschi et al.* [2004] and *Marone et al.*
¹¹⁴ [2004]. Although our models show a strong, high-velocity anomaly under the Hellenic
¹¹⁵ Arc at 60 - 150 km depths, related to the Dinarides-Hellenides subduction, the dip angle
¹¹⁶ is only poorly resolved. At 220 - 310 km depth, a high V_s -anomaly stretching along the
¹¹⁷ Southern Apennines up to Northern Italy is identified in the finite-frequency inversion,
¹¹⁸ while in the ray-theoretical model this anomaly seems to be shifted eastwards under the
¹¹⁹ Adriatic sea.

¹²⁰ Our estimated model error (Figure 2) is between 2% to 5%, obscuring most ray-theory
¹²¹ vs. finite-frequency discrepancies. Yet, error estimates from *Ekström et al.* [1997] are
¹²² conservative, and there are suggestive hints that the finite-frequency method is indeed
¹²³ enhancing resolution. With respect to the ray-theory solution, the finite-frequency one
¹²⁴ is more coherent with V_p structure found in a tectonic reconstruction of the temperature
¹²⁵ field [*de Jonge et al.*, 1994]: compare, e.g., Figure 3 (layer at 220 - 310 km) with fig.
¹²⁶ 6 of *Boschi et al.* [2004]. In the same depth range, a fast anomaly under the Central
¹²⁷ Alps, associated with past subduction, also found by *Schmid et al.* [2008], is reproduced
¹²⁸ more clearly in our finite-frequency model than in the ray-theoretical one: compare, in
¹²⁹ particular, our Tunisia-Central Europe cross-section of Figure 4 with fig. 8 of *Boschi et*
¹³⁰ *al.* [2004].

6. Conclusions

131 We inverted a new phase-anomaly database [Fry *et al.*, 2008] of intermediate to long-
132 period Rayleigh waves, confirming (at 150 s period) the presence of a distinct high-phase-
133 velocity zone between Southern Italy and the Hellenic Trench in finite-frequency inver-
134 sions, which is shifted to the Balkan coastline for ray-theoretical inversions. We con-
135 structed three-dimensional shear-velocity models by inverting dispersion curves, found at
136 each location in the European-Mediterranean region, from the previously obtained phase-
137 velocity maps derived by ray- and finite-frequency theory. In general, differences are
138 small compared to a conservative estimate of model error, but a tectonic reconstruction
139 [de Jonge *et al.*, 1994] of the region's temperature field supports our finite-frequency model.
140 Including dispersion measurements at shorter wave periods and basing the inversion on
141 refined models of the crust will allow to reduce the error bar on tomographic results, and
142 eventually quantify the improvement achieved via the finite-frequency approach.

143 **Acknowledgments.**

144 We thank John Woodhouse for giving us access to the large computational facility at
145 the Department of Earth Sciences, Oxford University. We also gratefully acknowledge
146 support from the European Commissions Human Resources and Mobility Programme,
147 Marie Curie Research Training Networks.

148

References

149 Bassin, C., G. Laske and G. Masters, 2000. The current limits of resolution for surface
150 wave tomography in North America, *Eos Trans. AGU*, **81**(F897).

- ¹⁵¹ Boschi, L. and G. Ekström, 2002. New images of the Earth's upper mantle from measure-
¹⁵² ments of surface wave phase velocity anomalies, *Journal of Geophysical Research-Solid*
¹⁵³ *Earth*, 107: p. 10.1029/2000JB000059.
- ¹⁵⁴ Boschi, L., G. Ekström and B. Kustowski, 2004. Multiple resolution surface wave tomog-
¹⁵⁵ raphy: the Mediterranean basin, *Geophysical Journal International*, 157: p. 293-304.
- ¹⁵⁶ de Jonge, M. R., M. J. R. Wortel and W. Spakman, 1994. Regional-Scale Tectonic Evolu-
¹⁵⁷ tion and the Seismic Velocity Structure of the Lithosphere and Upper-Mantle - the
¹⁵⁸ Mediterranean Region, *Journal of Geophysical Research-Solid Earth*, 99: p. 12091-
¹⁵⁹ 12108.
- ¹⁶⁰ Deschamps, F., S. Lebedev, T. Meier and J. Trampert, 2008. Stratified seismic anisotropy
¹⁶¹ reveals past and present deformation beneath the East-central United States, *Earth and*
¹⁶² *Planetary Science Letters*, in prep.
- ¹⁶³ Dziewonski, A. M. and D. L. Anderson, 1981. Preliminary Reference Earth Model, *Physics*
¹⁶⁴ *of the Earth and Planetary Interiors*, 25: p. 297-356.
- ¹⁶⁵ Ekström, G., J. Tromp and E. W. F. Larson, 1997. Measurements and global models of
¹⁶⁶ surface wave propagation, *J. Geophys. Res.*, 102, 8137-8157.
- ¹⁶⁷ Fry, B., 2007. *Surface wave tomography of the Mediterranean and central Europe: a new*
¹⁶⁸ *shear wave velocity model*, Ph.D. thesis, ETH Zurich, Switzerland.
- ¹⁶⁹ Fry, B., L. Boschi, G. Ekström and D. Giardini, 2008. Europe-Mediterranean tomography:
¹⁷⁰ High correlation between new seismic data and independent geophysical observables,
¹⁷¹ *Geophysical Research Letters*, 35: p. L04301.

- ¹⁷² Knopoff, L., 1972. Observation and inversion of surface-wave dispersion, *Tectonophysics*,
¹⁷³ 13(1-4), p. 497–519.
- ¹⁷⁴ Marone, F., S. van der Lee and D. Giardini, 2004. Three-dimensional upper-mantle S-
¹⁷⁵ velocity model for the Eurasia-Africa plate boundary region, *Geophysical Journal In-*
¹⁷⁶ *ternational*, 158: p. 109-130.
- ¹⁷⁷ Paige, C. C. and M. A. Saunders, 1982. Lsqqr - an Algorithm for Sparse Linear-Equations
¹⁷⁸ and Sparse Least-Squares, *Acm Transactions on Mathematical Software*, 8: p. 43-71.
- ¹⁷⁹ Panza, G. F., A. Peccerillo, A. Aoudia and B. Farina, 2007. Geophysical and petrological
¹⁸⁰ modelling of the structure and composition of the crust and upper mantle in complex
¹⁸¹ geodynamic settings: The Tyrrhenian Sea and surroundings, *Earth-Science Reviews*,
¹⁸² 80: p. 1-46.
- ¹⁸³ Peter, D., C. Tape, L. Boschi and J. H. Woodhouse, 2007. Surface wave tomography:
¹⁸⁴ global membrane waves and adjoint methods, *Geophysical Journal International*, 171:
¹⁸⁵ p. 1098-1117.
- ¹⁸⁶ Piromallo, C. and A. Morelli, 2003. P wave tomography of the mantle under the Alpine-
¹⁸⁷ Mediterranean area, *Journal of Geophysical Research-Solid Earth*, 108: p. 2065.
- ¹⁸⁸ Ritzwoller, M. H., Y. Yang, A.L. Levshin, E.R Engdahl and N.M. Shapiro, 2006. Thoughts
¹⁸⁹ on a European Seismic Reference Model: The role of surface waves from earthquakes
¹⁹⁰ and ambient noise, *Geophysical Research Abstracts*, 8: EGU06-A-05281.
- ¹⁹¹ Schmid, C., S. van der Lee, J. C. VanDecar, E. R. Engdahl and D. Giardini, 2008.
¹⁹² Three-dimensional S velocity of the mantle in the Africa-Eurasia plate boundary region
¹⁹³ from phase arrival times and regional waveforms, *Journal of Geophysical Research-Solid*

- ¹⁹⁴ *Earth*, 113: p. B03306.
- ¹⁹⁵ Schwab, F. and L. Knopoff, 1970. Surface-Wave Dispersion Computations, *Bulletin of the Seismological Society of America*, 60: p. 321-344.
- ¹⁹⁷ Shapiro, N. M. and M. H. Ritzwoller, 2002. Monte-Carlo inversion for a global shear-
¹⁹⁸ velocity model of the crust and upper mantle, *Geophysical Journal International*, 151:
¹⁹⁹ p. 88-105.
- ²⁰⁰ Spakman, W., S. van der Lee and R. van der Hilst, 1993. Travel-Time Tomography of the
²⁰¹ European Mediterranean Mantle down to 1400 Km, *Physics of the Earth and Planetary
202 Interiors*, 79: p. 3-74.
- ²⁰³ Tarantola, A., 2005. Inverse problem theory and methods for model parameter estimation,
²⁰⁴ *Philadelphia, PA: Society for Industrial and Applied Mathematics*.
- ²⁰⁵ Tesauro, M., M. K. Kaban and S. A. P. L. Cloetingh, 2008. Eucrust-07: A New Reference
²⁰⁶ Model for the European Crust, *Geophysical Research Letters*, 35: p. L05313.
- ²⁰⁷ Waldhauser, F., R. Lippitsch, E. Kissling and J. Ansorge , 2002. High-resolution teleseis-
²⁰⁸ mic tomography of upper-mantle structure using an a priori three-dimensional crustal
²⁰⁹ model, *Geophysical Journal International*, 150: p. 403414.
- ²¹⁰ Wortel, M. J. R., and W. Spakman, 2001. Subduction and slab detachment in the
²¹¹ mediterranean-carpathian region, *Science*, 291(5503), 437437.

Figure 1. Phase-velocity maps obtained from inversions based on numerical finite-frequency (top) and ray theory (bottom), from *Fry et al.* [2008] measurements at 40 s, 75 s, 150 s and 250 s.

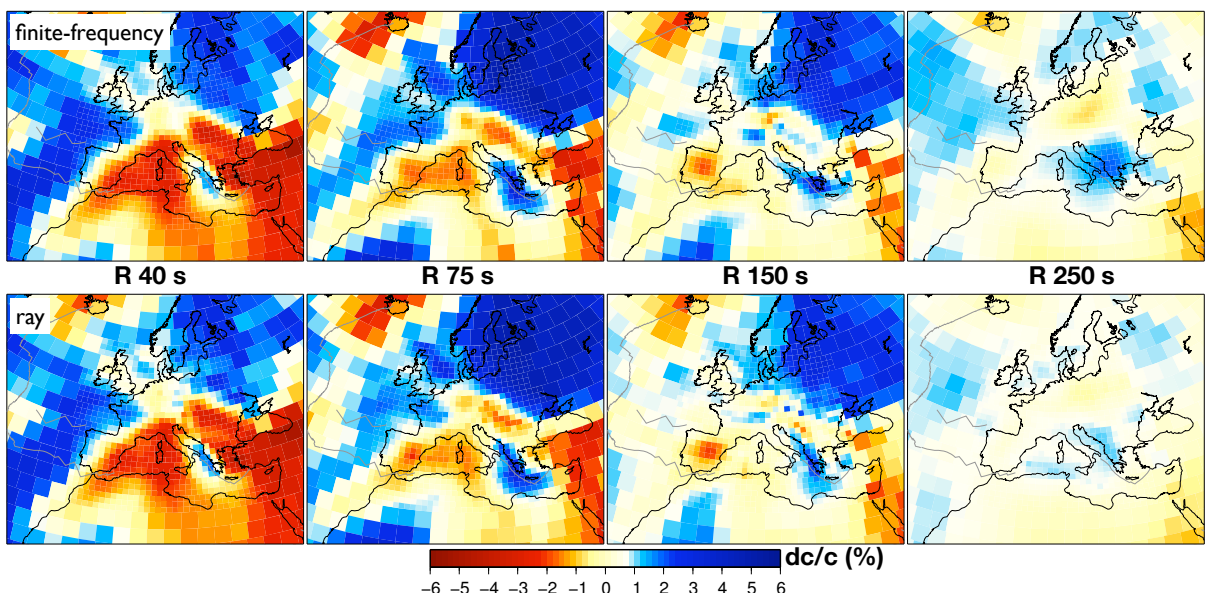


Figure 2. Local V_s profiles and their standard deviations (shaded areas). (a) Inversions from a “synthetic” dispersion curve computed from an artificial “input” profile (black line). Output profiles are obtained from a starting model with an upper-mantle PREM profile (gray dashed) and crustal structure fixed to either PREM (red) or the same crustal model used as input (blue). (b) Inversions from dispersion curves obtained from finite-frequency (green) and ray-theory (blue) maps (Figure 1) for a location in Southern Italy. The starting profile consists of a PREM mantle and crustal structure fixed to a combined Crust-2.0- and EuCrust-07-based model.

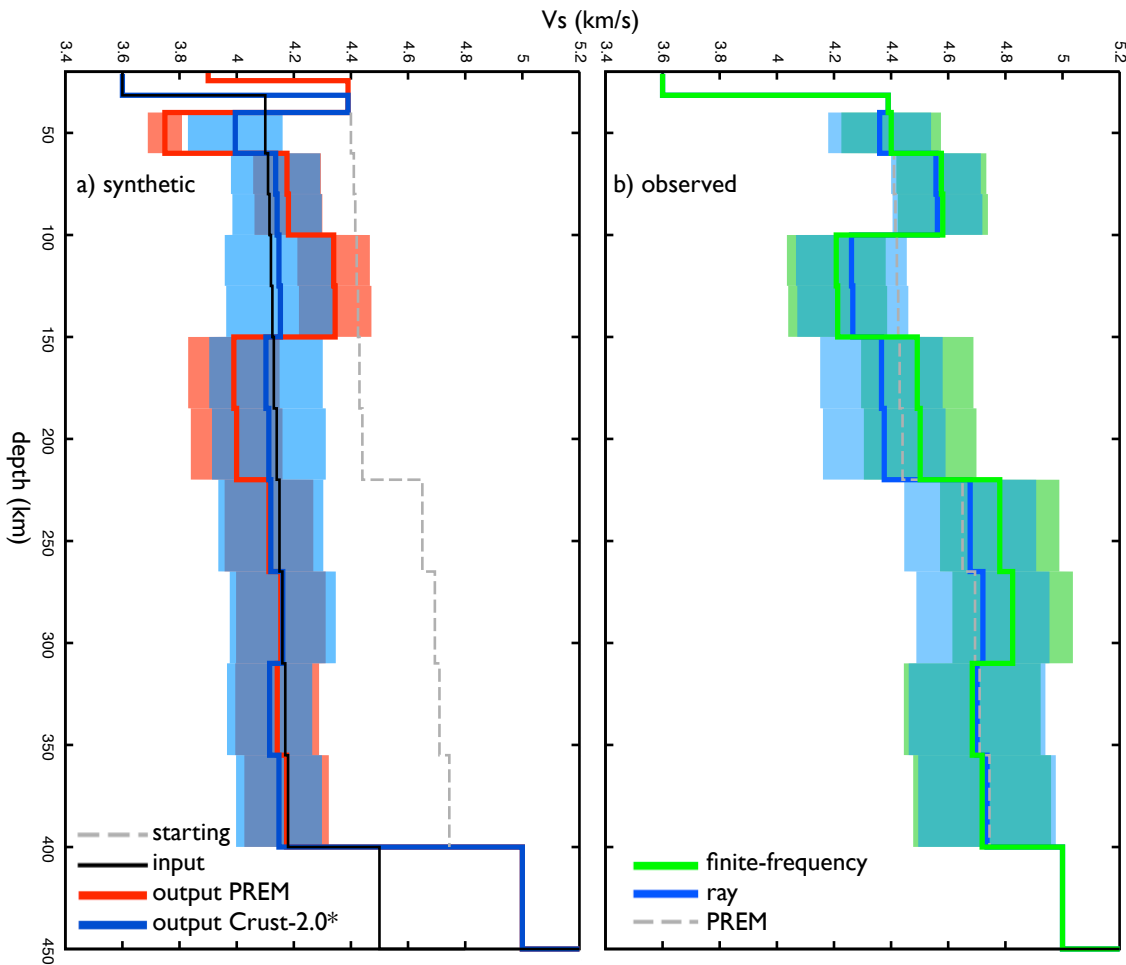


Figure 3. V_s perturbations (dVs) with respect to PREM at 60 - 100 km, 100 - 150 km, 150 - 220 km, 220 - 310 km and 310 - 400 km depths based either on finite-frequency (left) or ray-theoretically (right) derived dispersion curves. The standard deviations (STD) of the corresponding shear-velocity anomalies are given to the left of the models.

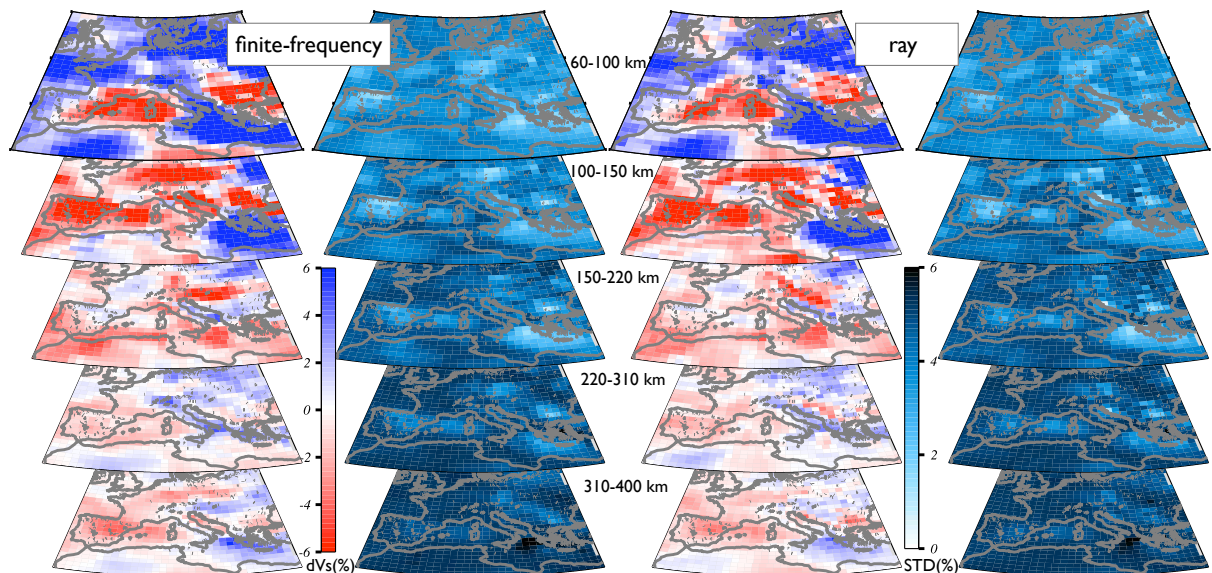


Figure 4. Perspective view of four different cross-sections through the finite-frequency shear-velocity model of Figure 3. The Tunisia-Central Europe cross-section also shows contour lines from the model of *Boschi et al.* [2004].

